



## 저작자표시-동일조건변경허락 2.0 대한민국

이용자는 아래의 조건을 따르는 경우에 한하여 자유롭게

- 이 저작물을 복제, 배포, 전송, 전시, 공연 및 방송할 수 있습니다.
- 이차적 저작물을 작성할 수 있습니다.
- 이 저작물을 영리 목적으로 이용할 수 있습니다.

다음과 같은 조건을 따라야 합니다:



저작자표시. 귀하는 원저작자를 표시하여야 합니다.



동일조건변경허락. 귀하가 이 저작물을 개작, 변형 또는 가공했을 경우에는, 이 저작물과 동일한 이용허락조건하에서만 배포할 수 있습니다.

- 귀하는, 이 저작물의 재이용이나 배포의 경우, 이 저작물에 적용된 이용허락조건을 명확하게 나타내어야 합니다.
- 저작권자로부터 별도의 허가를 받으면 이러한 조건들은 적용되지 않습니다.

저작권법에 따른 이용자의 권리는 위의 내용에 의하여 영향을 받지 않습니다.

이것은 [이용허락규약\(Legal Code\)](#)을 이해하기 쉽게 요약한 것입니다.

[Disclaimer](#)

공학석사 학위논문

**Structure Design and Functionalization  
Strategies of Silica Nanoparticle for Dual  
Modal Imaging and Specific Targeting**

생체 영상 및 특이적 표적을 위한  
다기능성 실리카 나노입자의 설계

2013년 2월

서울대학교 대학원

융합과학기술대학원

나노융합학과 전공

김 지 영

생체 영상 및 특이적 표적을 위한

다기능성 실리카 나노입자의 설계

**Structure Design and Functionalization**

**Strategies of Silica Nanoparticle for Dual**

**Modal Imaging and Specific Targeting**

지도 교수 이 윤 식

이 논문을 공학 석사 학위논문으로 제출함

2013 년 2월

서울대학교 대학원

융합과학기술대학원

나노융합학과

김 지 영

김지영의 석사 학위논문을 인준함

2013 년 2월

위 원 장 \_\_\_\_\_ (인)

부위원장 \_\_\_\_\_ (인)

위 원 \_\_\_\_\_ (인)

**Abstract**

**Structure Design and Functionalization  
Strategies of Silica Nanoparticle for Dual  
Modal Imaging and Specific Targeting**

Ji Young Kim

Graduate School of Convergence Science and Technology  
Seoul National University

Nanostructured materials exhibit unique and useful properties which can be applied to various areas. In particular, imaging science and technology has actively been adapting nanoparticles as imaging agents and tracking probes. Advances in imaging techniques allow for accurate detection of early-stage of cancer and targeted therapies based on the cancer-specific markers. However, among all the imaging modalities, no single modality is perfect to meet all the requirements in medical applications. Each imaging modality has certain advantages as well as limitations, and the choice for an imaging modality, or combination of techniques, is determined by the specific biological questions being asked. Developing dual modal imaging probes and combining the advantages of these modalities can offer synergistic advantages in providing more valuable diagnostic information and treatment strategies.

Hence, we demonstrated that multimodal imaging nanoparticle combined with optical imaging and nuclear imaging has merit for potential imaging of various biological targets and process with high sensitivity and specificity without the tissue penetrating limit. It is based on the use of fluorescent dye-doped silica nanoparticles (F-silica NPs) as the core material of optical

imaging contrast agent. The silica NPs have the advantages that their surface can be easily modified according to applications. Furthermore, we have also conjugated the well-known PET imaging probe  $^{68}\text{Ga}$  and targeting moiety, Herceptin on the F-silica NPs, which will allow specific targeted bio imaging independent of tissue depth. This multifunctional nanoprobe is capable of optical imaging which is also detectable by PET after cell targeting.

Moreover, in order to impart stealth properties to the F-silica NPs, we conjugated heterobifunctional PEG on F-silica NPs. Also we confirmed the effect of PEG chain length on the resulting particle size, surface charge and  $^{68}\text{Ga}$  labeling efficiency of F-silica NPs. The method of using PEG 10,000 on 1 v/v% APTS modified F-silica NPs was effective surface modification strategy for effective  $^{68}\text{Ga}$  labeling. Therefore, functionalized F-silica NPs are promising candidate as an efficient imaging probe of PET technique. We will further discuss the strategy of ligand conjugation for targeting without losing its functionality after attachment to the F-silica NPs.

**Keywords: multifunctional nanoparticle, F-silica NPs, dual modal imaging, targeted imaging probe, surface modification**

**Student Number: 2010-22665**

# Contents

Chapter 1 Introduction .....	1
1.1 Imaging Modalities for Bio Imaging .....	1
1.2 Multifunctional Nanoparticles for Multimodal Imaging .....	4
1.3 Silica Nanoparticles-based Targeted Imaging Probe .....	6
1.4 Surface Engineering Strategies for <i>In vivo</i> Imaging .....	8
1.5 Research objective .....	9
 Chapter 2 Experimental.....	 11
2.1 General .....	11
2.1.1 Material.....	11
2.1.2 Instruments.....	12
 2.2 Synthesis of F-silica NPs .....	 13
2.2.1 Preparation of FITC-APTS Conjugates .....	13
2.2.2 Synthesis of F-silica NPs .....	13
 2.3 Surface modification of F-silica NPs .....	 14
2.3.1 Preparation of Amine-modified F-silica NPs.....	14
2.3.2 Preparation of PEG modified F-silica NPs .....	15
2.3.3 NOTA and Water soluble linker Conjugation to F-silica NPs	16
2.3.4 Antibody Conjugation of F-silica NPs.....	17

2.3.4.1. Preparation of Half Fragmented Herceptin.....	17
2.3.4.2. Herceptin Immobilization on F-silica NPs .....	17
2.3.5 Labeling with $^{68}\text{Ga}$ .....	18
2.3.6 <i>In vitro</i> Cellular Binding .....	18
 Chapter 3 Results and Discussion .....	19
3.1 Synthesis of F-silica NPs .....	19
3.2 Preparation and Characterization of Surface modified F-silica NPs .....	22
3.2.1 Preparation of Amine-modified F-silica NPs .....	22
3.2.2 Preparation of PEG modified F-silica NPs .....	26
3.2.3 Preparation and Characterization of Multifunctional F-silica NPs .....	29
3.2.4 Radio-labeling Surface Modified F-silica NPs .....	32
3.2.5 Aggregation Studies of Multifunctional F-silica NPs .....	34
3.2.6 <i>In vitro</i> Cellular Binding .....	37
 Conclusion.....	39
 Abstract .....	40
 References .....	42

## List of Tables

Table 1.1	Comparison of Commonly used Bioimaging Techniques .....	5
Table 3.1	Quantifications of Amine Moieties on the F-silica NPs .....	23
Table 3.2	The Results of DLS Analysis Data with Size and Zeta Potential of Multifunctional F-silica NPs .....	31
Table 3.3	$^{68}\text{Ga}$ Labeling Efficiency of Multifunctional F-silica NPs .....	33
Table 3.4	The Results of DLS Analysis of Multifunctional F-silica NPs after $^{68}\text{Ga}$ Labeling .....	33



## List of Figures

Figure1.1	Multifunctional Nanoparticles for Multimodal Imaging and Theragnosis .....	3
Figure 3.1	Preparation of F-silica NPs by Reverse Microemulsion Method	21
Figure 3.2	TEM Images of Synthesized F-silica NPs .....	21
Figure 3.3	TEM Images of Amine Modified F-silica NPs.....	24
Figure 3.4	Scheme of Surface Modification for Fabrication Multifunctional F-silica NPs .....	25
Figure 3.5	TEM Images of PEGlyated F-silica NPs .....	27
Figure 3.6	The TGA Analysis Data of PEG Modified F-silica NPs.....	28
Figure 3.7	The CLSM Images of Dispersed Multifunctional F-silica NPs..	35
Figure 3.8	Confocal Images of Functionalized F-silica NPs .....	38

# Chapter 1. Introduction

## 1.1. Imaging Modalities for Bio Imaging

Bio imaging has become an indispensable tool in biomedical research. Advances in imaging techniques allow accurate mapping of lesions improving preoperative planning and patient selection. Also it attempts to characterize and quantify biological processes at the cellular and subcellular level in intact living subjects. A number of molecular imaging techniques, such as optical imaging (OI), magnetic resonance imaging (MRI), ultrasound imaging (USI), positron emission tomography (PET), and others have been reported for imaging of *in vitro* and *in vivo* biological specimens. These imaging system provides anatomical and physiological information.<sup>1</sup>

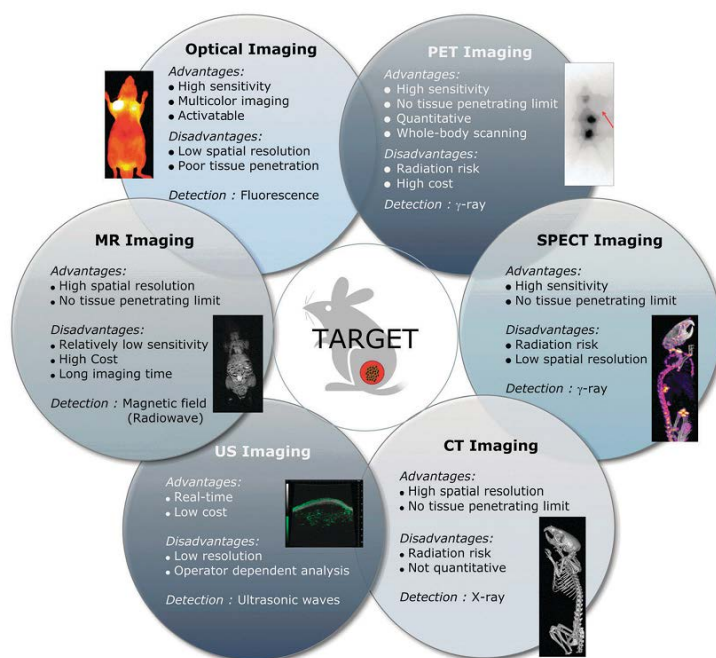
OI is a relatively low-cost, noninvasive and extensively used imaging technique, in that light is taken as the most readily available and versatile imaging radiation source in nature. Fluorescence imaging and bioluminescence imaging are two major techniques in OI to analyze the propagation of nonionizing radiation, light photons through a medium such as tissue.<sup>2</sup> Today, tomographic reconstruction of infrared photons, spectral unmixing, image fusion and multichannel imaging have become routine, and several preclinical and clinical imaging systems are commercially available.<sup>3</sup>

Current *in vivo* cancer imaging techniques such as MRI and CT are

suitable for providing spatial information and thus capable of identifying anatomical location of tumor. CT is based on the exploitation of X-ray scanning, its attenuation in tissues and computed image reconstruction to obtain morphologic and vascular information within the body. MRI is a noninvasive medical diagnostic technique. MRI has high spatial resolution of image and combines morphological and functional imaging. However the sensitivity of these techniques is not significantly high enough for detecting abnormalities at the cellular level.

On the other hand, PET provides high target sensitivity and three-dimensional images of various biochemical functions in human body. But this modality suffers from poor spatial resolution.<sup>4</sup>

Among all the molecular imaging modalities, no single modality is perfect to meet all the requirements in medical applications. Each imaging modality has certain advantages as well as limitations, and the choice for an imaging modality, or combination of the techniques, is determined by the specific biological questions being asked. Developing dual modal imaging probes and combining the advantages of these modalities can offer synergistic advantages in providing more valuable diagnostic information and treatment strategies.<sup>5</sup>



**Figure 1.1.** Multifunctional Nanoparticles for Multimodal Imaging and theragnosis<sup>6</sup>

## 1.2. Multifunctional Nanoparticles (NPs) for Multimodal Imaging

Nanostructured materials exhibit unique and useful unique electric, optical, and magnetic properties which can be applied to various areas. In particular, imaging science and technology has actively been adapting nanoparticles as imaging agents and tracking probes. Due to the large surface area of nanoparticles and inherent functionalities, structural modifications are readily achieved to alter their pharmacokinetics, their vascular circulation life-time, improve their extravasation capacity, and ensure an enhanced biodistribution *in vivo*. Many nanoparticle-based structures are currently under investigation and some well-studied nanoparticles include silica nanoparticles, quantum dots, iron oxides, dendrimers, nanotubes and so on.<sup>7</sup> For example, proteic fluorophores and organic/inorganic fluorescent dyes are popular imaging agents. Besides, quantum dots and silica nanoparticles with fluorescent shell structure have also been employed as fluorescent imaging agents *in vitro* and *in vivo*. Commonly used contrast agents for MRI include paramagnetic complex, paramagnetic ion nanoparticles, superparamagnetic iron oxide nanoparticles.<sup>8</sup>

Gold NP-based contrast agents have drawn substantial interest *in vivo* X-ray imaging for the last decade. These particles have shown to have *in vivo* functionality as CT contrast agents for cancer. Gold NPs are currently being explored in multiple clinical trials.

PET and SPECT are two major type of radionuclide imaging modalities. Various radionuclides, such as  $^{16}\text{F}$ ,  $^{64}\text{Cu}$  and  $^{68}\text{Ga}$  (for PET) and  $^{125}\text{I}$  and  $^{111}\text{In}$  (for SPECT) can be applied as radioisotopes, respectively.<sup>9</sup>

Various nanoparticles are used as imaging probes. Although it is challenging to integrate dual or multimodal imaging properties into single probe, this concept is probably the most promising approach to overcome current drawbacks in one single imaging modality. Nowadays, many nanoparticles-based dual or multimodal imaging probes have been developed and applied to multimodal imaging in living systems.

**Table 1.1.** Comparison of Commonly used Bioimaging Techniques<sup>7</sup>

Technique	Typical NP table	Advantages	Disadvantages
OI	QDs, dye-doped NPs, upconverting NPs, SWNTs and other carbon-based nanomaterials	High-throughput screening High sensitivity	Limited clinical translation Low depth penetration
MRI	Iron oxide NPs, Gd-doped NPs and hyperpolarized probes (e.g., $^{129}\text{Xe}$ )	Clinical translation High resolution	Costs Imaging time
PET	NPs incorporating radioisotopes (e.g., $^{18}\text{F}$ , $^{11}\text{C}$ , $^{64}\text{Cu}$ , $^{124}\text{I}$ , $^{68}\text{Ga}$ )	Clinical translation High sensitivity	Costs
CT	Iodinated NPs, gold NPs, iron oxide-doped nanomaterials	High spatial resolution Clinical translation	No target-specific imaging Poor soft contrast
SPECT	NPs incorporating radioisotopes (e.g., $^{99\text{m}}\text{Tc}$ , $^{111}\text{In}$ )	Clinical translation Unlimited depth penetration	Limited spatial resolution
US	Microbubbles, nanoemulsions, silica NPs, polystyrene NPs	Clinical translation High spatial and temporal resolution	Operator dependency

### 1.3. Silica Nanoparticles-based Imaging Probe

Silica based nanoparticles(NPs) have been developed for the purposes of bioimaging and biosensing. Silica is a good material for this work because it is easy to host imaging agents such as fluorescent dyes, metal ions, and drugs. Silica matrix is transparent and allows for excitation and emission light to pass through efficiently. Encapsulation by silica also provides enhanced photostability for optical agents.<sup>10</sup> The surface of silica particles can be modified easily to attach bio molecules; it is water dispersible, resistant to microbes, biocompatible and resistant to swelling in various solvents. These characteristics of silica have led to its use as several multifunctional nanoparticles. These silica NPs are used in fluorescence imaging as dye-doped silica NPs. Commonly, rapid photobleaching is one of the problems with organic dyes. Encapsulation of dyes in a silica matrix is one method presently used to maximize both *in vitro* and *in vivo* stability. This minimizes oxygen access, increases chemical stability, photostability (suitable of imaging studies at cellular, subcellular, and even molecular level) and allows surface modification to enhance hydrophilic character and to attach biomolecules.<sup>11</sup> Therefore, silica NPs can improve the ability of fluorescence dyes to perform cellular imaging and targeting.

Meanwhile, the development of targeted contrast agents for bio imaging has made it possible to selectively view specific biological

events and process in both living and nonviable systems with improved detection limits, imaging modalities and engineered biomarker functionality.<sup>12</sup> There is a need, above all, to develop novel NPs for accurate detection of early-stage of cancer and for targeted therapies based on the cancer-specific markers, which could lead to personalized medicine. Recent advances in nanomaterials have great potential targeting imaging probe. Several ligands with therapeutic and diagnostic properties can be incorporated on the NP's surface. Multivalent targeting significantly increases the binding affinity of a NPs toward a target cell.<sup>13</sup> The targeted delivery of nanomaterials can overcome problems associated with conventional anticancer drugs, including insolubility in aqueous conditions, rapid clearance, and a lack of selectivity, resulting in nonspecific toxicity toward normal cells.<sup>14</sup> The silica NPs are optically transparent, water dispersible, biologically inert, nontoxic, and have well established conjugation strategies to modify the surface using silane chemistry.<sup>15</sup> Especially, the advanced features of silica NP probes can afford a substantial advantage in detection of single molecule, bioimaging and extraction of cell and cellular components, as well as disease targeting.



## **1.4. Surface Engineering of Nanoparticles for *in vivo* Imaging**

NPs can be used as powerful probes for *in vivo* imaging in medical and biological diagnostics. Several NP-based contrast agents have been developed to overcome the issues of conventional contrast agents. However, most of the currently developed NP probes are limited to a single imaging modality. Target specificity, noninvasiveness, high spatial resolution, 3-D tomography and real-time imaging are the important requirements for NPs to be used in biomedical application. But, a single imaging modality alone can not possess all the necessary requirements.<sup>16</sup> Therefore, multimodal imaging strategy can compensate for the weakness of single imaging modality. For multimodal NPs fabrication, the integration of multi-components into a NP can be achieved by modifying the NP's surface, and then combining different modalities into a single system. The surface of NPs can accommodate a large number or a wide range of surface functional groups allowing conjugation of diagnostic and therapeutic agents as well as targeting moieties.<sup>17</sup>

## 1.5. Research Objective

A current approach to overcome the limitations imposed by a single imaging modality is to combine two or more modalities into a single NP. For example, a core NP could be linked to a specific targeting ligand that recognizes their target cells. Simultaneously, the same particle can be coupled with an imaging agent for multimodal imaging or a moiety to evaluate the therapeutic efficacy of a drug or a therapeutic agent. In short, the function of the multifunctional nanoparticle depends on the component attached.<sup>18</sup> Hence, we expect that multimodal NPs combined with optical imaging and nuclear imaging have merit for potentially imaging of various biological targets and process with high sensitivity and specificity without the tissue penetrating limit. It is based on the use of fluorescent dye-doped silica NPs as the core material for optical imaging. The silica NPs have the advantages that their surface can be easily modified according to applications. These characteristics of silica NPs have provided an efficient platform for multifunctional nanoprobe. Furthermore, we have also conjugated the well-known PET imaging probe  $^{68}\text{Ga}$  and targeting moiety, Herceptin to the F-silica NPs, which will allow specific targeting and bio imaging. For this purpose, we have designed a conjugation method of radioactive  $^{68}\text{Ga}$  chelator, NOTA on F-silica NPs. Also, Herceptin, antibody of HER2, was chosen as the targeting moiety of multifunctional nanoprobe. Overexpression of HER2 protein

has been observed on the plasma membrane of tumors, in particular breast and ovarian cancers. Herceptin conjugated multifunctional Si NPs can be used as a HER2-targeting diagnostic imaging probe. This multifunctional nanoprobe is capable of optical imaging and detectable by PET after cell targeting. Furthermore, in order to impart stealth properties to the NPs, heterobifunctional PEG was conjugated to F-silica NPs. PEG is commonly used to achieve stealth properties, due to its hydrophilicity, flexibility, which help the NPs to be dispersed and to increase their blood circulation times.<sup>19-20</sup>

We hope that F-silica NP based multifunctional imaging probes for specific targeting will be used as dual modality molecular imaging probes.

## Chapter 2. Experiments

### 2.1. General

#### 2.1.1. Material

3-(Aminopropyl)triethoxysilane (APTS), Rhodamine B isothiocyanate (RBITC), triton X-100, tetraethoxyorthosilicate (TEOS), ethylenediaminetetraacetic acid (EDTA), 2-mercaptoethylamine HCl (2-MEA), (3-trihydroxysilyl)propyl methyl phosphonate monosodium salt (THPMP, 24 wt% solution in water) were purchased from Sigma-Aldrich (St. Louis, MO, USA). Cyclohexane and n-hexanol were bought from Junsei Chemicals (Tokyo, Japan). Ammonium hydroxide (NH<sub>4</sub>OH, 27%), ethanol, *N*-methyl-2-pyrrolidone (NMP), dimethylformaldehyde (DMF), piperidine were purchased from Dae-Jung Chemicals (Siheung, Korea). Fmoc-Lysine was bought from Bachem (Torrance, USA). (Benzotriazol-1-yloxy)-tris(dimethylamino)-phosphonium hexafluorophosphate (BOP), 1-hydroxybenzotriazole (HOBt) were purchased from Bead Tech (Seoul, Korea). *N,N*-Diisopropyl ethylamine (DIEA) was bought from Alfa Aesar (Massachusetts, USA). Fmoc protected polyethylene glycol active ester (MW 10000) was purchased from Creative PEGWorks (Winston Salem, USA). 1,4,7-Triazacyclononane-1,4,7-triacetic acid (NOTA), 3-sulfo-*N*-hydroxysuccinimidyl-4-(*N*-maleimidomethyl)cyclohexane-

1-carboxylate sodium salt (sulfo-SMCC) was bought from Thermo scientific (IL, USA). Trastuzumab (Herceptin) was purchased from Roche (Seoul, Korea).

### **2.1.2. Instruments**

Transmission electron microscope (TEM) images were obtained using Energy-Filtering transmission electron microscope (Carl Zeiss, LIBRA 120, Germany). The particle size was measured using a particle size analyzer, Zetasizer Nano S (Malvern Instruments, Malvern, UK). The zeta potential was measured by using a Zetasizer Nano Z (Malvern Instruments). TGA analysis was performed by using Thermo Gravimetric Analyzer (TGA; TA Instruments, Q-5000 IR, USA).  $^{68}\text{Ga}/^{68}\text{Ga}$  generator was purchased from Cyclotron (Obninsk, Russia). Instant TLC-silica gel (ITLC-SG) plates were bought from Pall (USA). Radio-thin layer chromatography (TLC) was counted using a Bio-Scan AR-2000 System imaging scanner (Bioscan, USA) .

Fmoc quantification test was followed by UV/visible spectrophotometer (Mecasys Co. Ltd., Optizen 2120 UV).

## **2.2. Synthesis of F-silica NPs**

### **2.2.1. Preparation of FITC-APTS Conjugates**

FITC (3.5 mg) was dissolved in 500  $\mu\text{L}$  of absolute ethanol and then 3.6  $\mu\text{L}$  of APTS was added and shaken under dark atmosphere for 18 hr.

### **2.2.2. Synthesis of F-silica NPs**

A water in oil reverse microemulsion was prepared by mixing 17.7 mL of Triton X-100, 18 mL of *n*-hexanol (co-surfactant), 77 mL of cyclohexane (oil phase), and 4 mL of DI water in a 250 mL glass container for 15 min at RT. And then FITC-APTS conjugates were added. After 10 min of stirring, 1 mL of silica precursor, TEOS and 1.2 mL of  $\text{NH}_4\text{OH}$  were added to the microemulsion solution. After 30min of stirring, 150  $\mu\text{L}$  of THPMP was added and stirring was continued at RT for 20 hr. After 20 hr, the microemulsion system was broken by adding 40 mL of ethanol, and F-silica NPs were separated from the microemulsion by centrifugation. F-silica NPs were then repeatedly washed and centrifuged 5 times ethanol by votexing and sonication.

## **2.3. Surface Modification of F-silica NPs**

### **2.3.1. Preparation of Amine-modified F-silica NPs**

To prepare amino group modified F-silica NPs, F-silica NPs were first treated with APTS. A 50  $\mu$ L of 5 v/v% APTS was added to 1 mL of F-silica NPs dispersed in ethanol (25 mg/mL). Then, 10  $\mu$ L of  $\text{NH}_4\text{OH}$  was added to the mixture. The mixture was stirred for 1 hr at 50  $^{\circ}\text{C}$ . The mixture was then purified by centrifugation (14000 rpm for 30 min) and decantation (5 times) in NMP.

The amino group of F-silica NPs was coupled with Fmoc-Lys for increasing the amino group moiety. To the previously prepared amine modified F-silica NPs (1 eq.) in NMP, Fmoc-Lys (3 eq.) was coupled with HOBt (3 eq.), BOP (3 eq.) and DIEA (3 eq.) in NMP at RT for 2 hr. After Fmoc group deprotection with 20 % piperidine in NMP for 10 min, Fmoc-Lys was coupled again to Lys modified F-silica NPs with HOBt (3 eq.), BOP (3 eq.) and DIEA (3 eq.) in NMP. The mixture was stirred at RT in 2 hr and then purified by centrifugation (14000 rpm for 30 min) 5 times.

### 2.3.2. Preparation of PEG Modified F-silica NPs

To prepare biocompatible NPs, F-silica NPs functionalized with amino groups was react with heterobifunctional PEG (Fmoc-PEG-COOH) of two different chain lengths (molecular weight of PEG = 2000 and 10000, respectively). The carboxyl group of Fmoc-NH-PEG<sub>2000</sub> (3 eq.) was coupled to amino groups on F-silica NPs (1eq.) with HOBt (3 eq.), BOP (3 eq.) and DIEA (3 eq.) in NMP for 2 hr at RT. In another case, Fmoc protected PEG<sub>10000</sub> (3 eq.) with active ester group was added to 10 mg of amine functionalized F-silica NPs dispersed in NMP, followed by addition of DIEA into the mixture. The mixture stirred for 5 hr at RT.

After deprotection of Fmoc group, PEGylated F-silica NPs were coupled with Fmoc-Lys (3 eq.) with HOBt (3 eq.), BOP (3 eq.) and DIEA (3 eq.) in NMP for 2 hr at RT to prepare amino groups on the surface of F-silica NPs. The resulting mixture was treated with 20 % of piperidine in NMP for deprotection of Fmoc group.



### **2.3.3. NOTA and Water soluble linker Conjugation to F-silica NPs**

To the previously prepared amino functionalized F-silica NPs were added a mixture of SCN-NOTA (5 eq.) and water-soluble linker sulfo-SMCC (5 eq.) in PBS buffer solution (pH 7.5) and incubated for 5 hr at RT. The isothio cyanate group of  $^{68}\text{Ga}$  chelator, *p*-SCN-Bn-NOTA, was then reacted with the amine-functionalized F-silica NPs. On the other hand, carboxyl group of sulfo-SMCC was bonded to amine group of F-silica NPs, which form an amide linkage. And then the mixture was purified with unconjugated NOTA and SMCC by centrifugation (14000 rpm for 30min) 5 times.

## **2.3.4. Antibody Conjugation of F-silica NPs**

### **2.3.4.1. Preparation of Half Fragmented Herceptin**

A 24  $\mu\text{L}$  of MEA (6 mg/mL) and 50  $\mu\text{L}$  of EDTA (1 mg/mL) in PBS buffer (pH 7.5) solution were added into 240  $\mu\text{g}$  of half fragment Herceptin in PBS buffer (pH 7.5) solution and then mixture was incubated for 90 min at  $37^\circ\text{C}$ . The half fragmented Herceptin was separated from the resulting mixture using PD-10 desalting column.

### **2.3.4.2. Herceptin Immobilization on F-silica NPs**

For the coupling reaction, the prepared F-silica NPs suspension was incubated with the half fragmented Herceptin in PBS buffer (pH 7.5) solution, to achieve a covalent linkage between antibody and the nanoparticle system. The incubation was performed for 2 hr at RT under constant shaking.

### **2.3.5. Labeling with $^{68}\text{Ga}$**

$^{68}\text{GaCl}_3$  in 0.1 N hydrochloride acid was obtained from an eluent of  $^{68}\text{Ga}/^{68}\text{Ga}$  generator. Radiolabeling of all F-silica NPs (250  $\mu\text{g}$  each) was carried out at pH 8 solution with 1 mL of  $^{68}\text{GaCl}_3$  and 220  $\mu\text{L}$  of 1 M sodium acetate (pH 5.6). Then the reaction mixtures were incubated at 37 °C for 30 min. The labeling yield was determined by Instant Thin-Layer Chromatography (ITLC-SG) in 0.1 M citric acid. The strip was counted using a TLC scanner (AR-2000; Bioscan, USA).

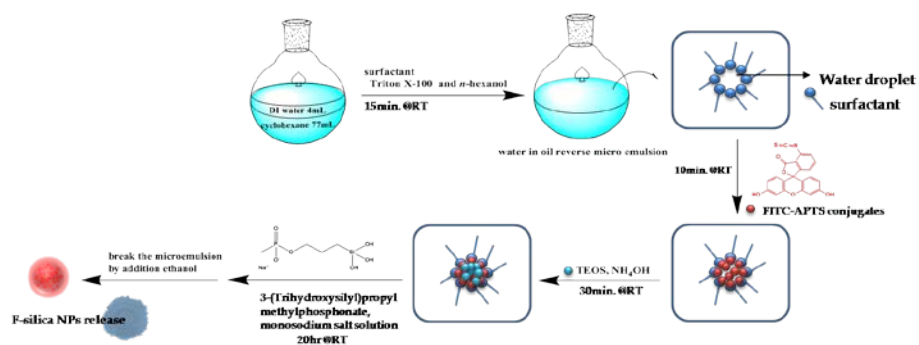
### **2.3.6. *In vitro* Cellular Binding**

The glass cover slips with breast cancer cell lines (SKBR3<sup>+++</sup>) on them were removed from the culture medium and placed in the microscope chamber at 4 °C. The cells were covered with DPBS solution and surface modified NPs (1mg/mL). After the cells were incubated with the NPs for 30 min, the cell images were taken to monitor cellular binding of NPs.

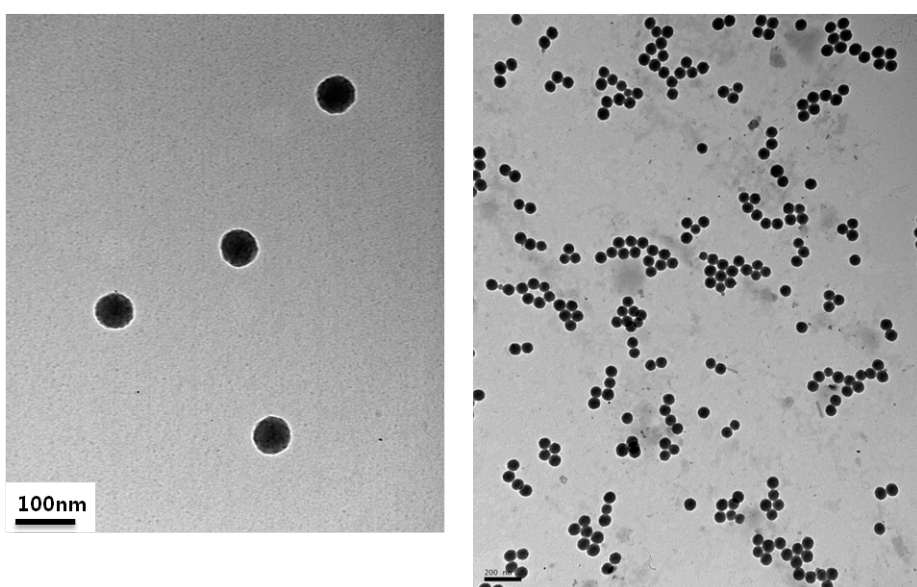
## **Chapter 3. Results and Discussion**

### **3.1. Synthesis of F-silica NPs**

As illustrated in Figure 3.1, monodisperse fluorescent dye doped silica NPs were synthesized using water in oil reverse microemulsion system. Reverse microemulsion methods create thermodynamically stable nanodroplet of amphiphilic surfactants. The nano-droplets of water in oil phase act as a reactor for discrete particle formation. This method has been known to be efficient for the fabrication of highly monodispersed spherical microparticles and for easy surface modification.<sup>21</sup> It was reported that phosphonate ligand groups on the particle's surface gave highly negative zeta potential so that NPs could be well dispersed.<sup>22</sup> Zeta potential of the synthesized F-silica NPs was -20.3 mV and hydrodynamic size was 89.5 nm (The size of F-silica NPs was 70 nm in diameter as determined by TEM). As expected, TEM images showed that the synthesized F-silica NPs were well dispersed and revealed spherical structures having monodispersity.



**Figure 3.1.** Preparation of F-silica NPs by Reverse Microemulsion method.



**Figure 3.2.** TEM Images of Synthesized F-silica NPs.

## **3.2. Preparation and Characterization of Surface Modified F-silica NPs**

### **3.2.1. Preparation of Amine-modified F-silica NPs**

The F-silica NPs were modified with amino groups for the conjugation of various molecules. In order to introduce amino group, F-silica NPs were functionalized with APTS. The amino group is a key surface-bound, functional group for the immobilization of chemicals and biological molecules. As expected, the more APTS was added into F-silica NPs, the less negative charge was developed on the F-silica NP's surface. (1 v/v% APTS, -16.4; 5 v/v% APTS, -13.5).

For increasing the amino group content, Lysine (Lys) was coupled to the amine-modified F-silica NPs twice. Lys has two amino groups. Consequently, Lys modified F-silica NPs can have double the amount of amino groups. After Fmoc-Lys was coupled to the amino group of F-silica NPs, we quantified the amino groups by Fmoc titration. Table 3.2 summarizes the results of the amino group quantification, which shows that the amount of amino group on Lys modified F-silica NPs was actually increased to double (from 70.4 to 146.9  $\mu\text{mol/g}$ ) after coupling of Lys. Therefore, Lys coupling turned out to be an efficient method for increasing amino group.

**Table 3.1.** Quantifications of Amino Groups on the F-silica NPs

**(a) After 1<sup>st</sup> Lys coupling**

F-silica(mg)	3	7	15
UV abs.	0.178	0.383	0.646
	0.183	0.394	0.656
	0.191	0.477	0.664
average	0.184	0.418	0.655

amine moiety	78.63	76.56	56.01
( $\mu\text{mol/g}$ )			
average	70.40	$\mu\text{mol/g}$	

**(b) After 2<sup>nd</sup> Lys coupling**

F-silica(mg)	3	7	15
UV abs.	0.376	0.84	1.404
	0.385	0.841	1.424
	0.398	0.844	1.435
average	0.386	0.842	1.421

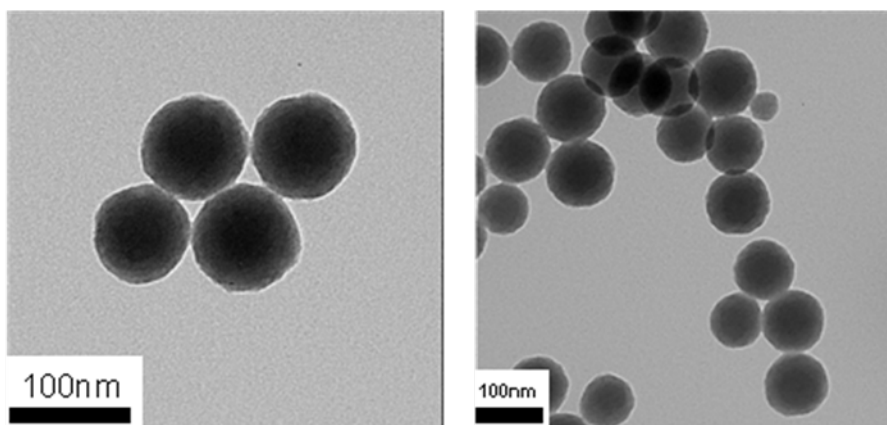
amine moiety	165.10	154.15	121.45
( $\mu\text{mol/g}$ )			
average	146.90	$\mu\text{mol/g}$	

(a) Quantification after first coupling of Lys

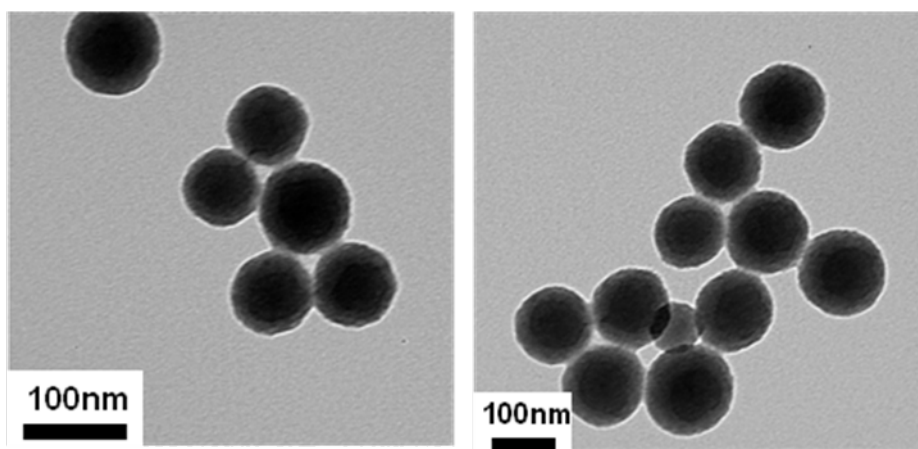
(b) Quantification after second coupling of Lys



**(a)**

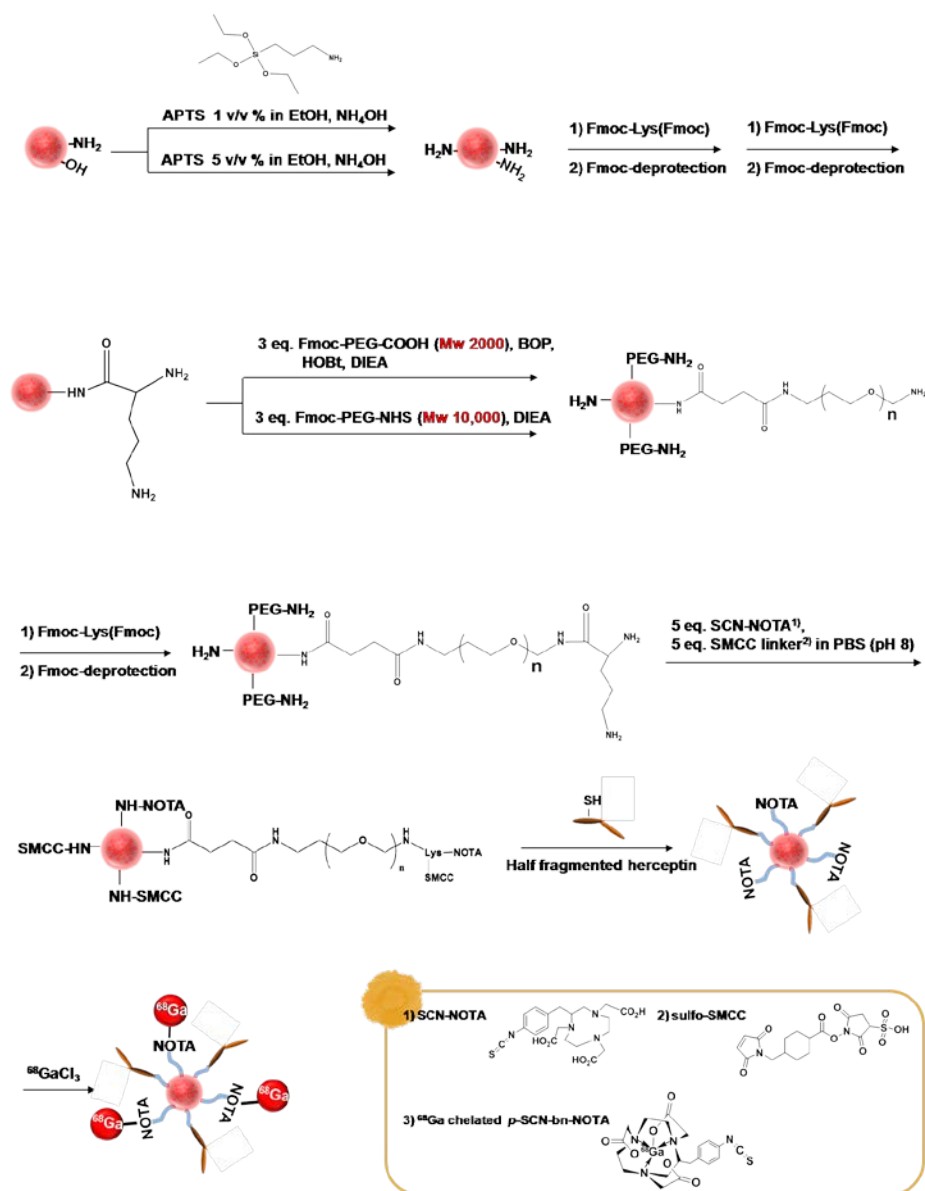


**(b)**



**Figure 3.3.** TEM images of amine modified F-silica NPs ;

(a) after APTS treatment , (b) after Lys coupling



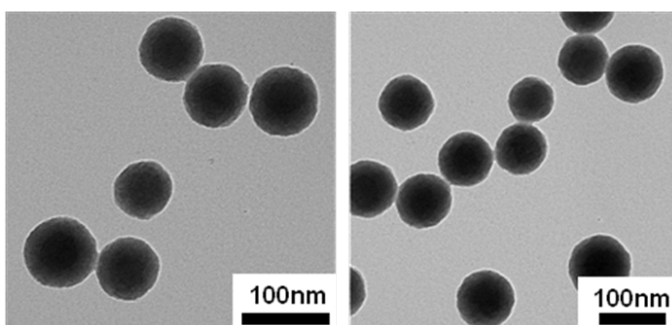
**Figure 3.4.** Scheme of surface modification for fabrication multifunctional F-silica NPs.

### 3.2.2. Preparation of PEG modified F-silica NPs

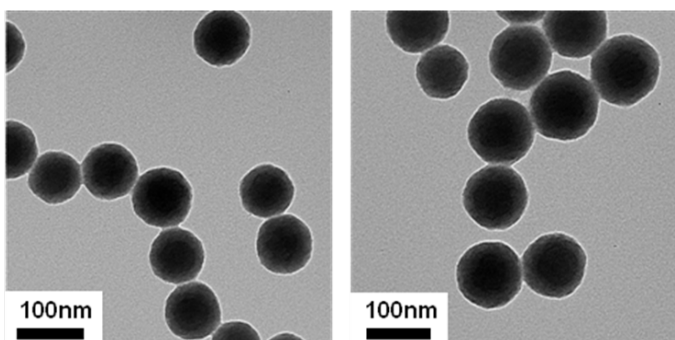
In general, nanoparticles tend to aggregate through hydrophobic interactions or van der Waals forces in an effort to minimize the surface energy. In the blood stream, such aggregates can trigger opsonization, a process by which a particle is covered with opsonin proteins, thereby making it more visible to the mononuclear phagocytic system (MPS), such as RES. The phagocytic mechanisms render nanoparticles ineffective as theragnostic vehicles by removing them from the bloodstream.<sup>23</sup> In order to give stealth properties to the nanoparticles, one of the most promising method is PEGylation, modification with PEG. It was reported that PEG molecules interfere with the binding of opsonin proteins to the nanoparticle surfaces, supporting long circulation time, thereby increasing the chance that the nanoparticles can effectively target tumor sites.<sup>24</sup>

Covalent attachment of one end of a heterobifunctional PEG to the amino groups on the F-silica NPs was tried. The configuration and the effect of the PEG layer are dependent on the PEG chain length and their surface density. We investigated the effect of PEG chain length on the resulting NPs's size, surface charge and <sup>68</sup>Ga labeling efficiency of NPs. We chose the PEG chains having two different chain lengths (MW of 2000 and 10,000, respectively). The amount of loaded PEG<sub>2000</sub> on the F-silica NPs was 6.5 wt%, which was analyzed by TGA. In the case of PEG<sub>10000</sub>, it was 11.7 wt%.

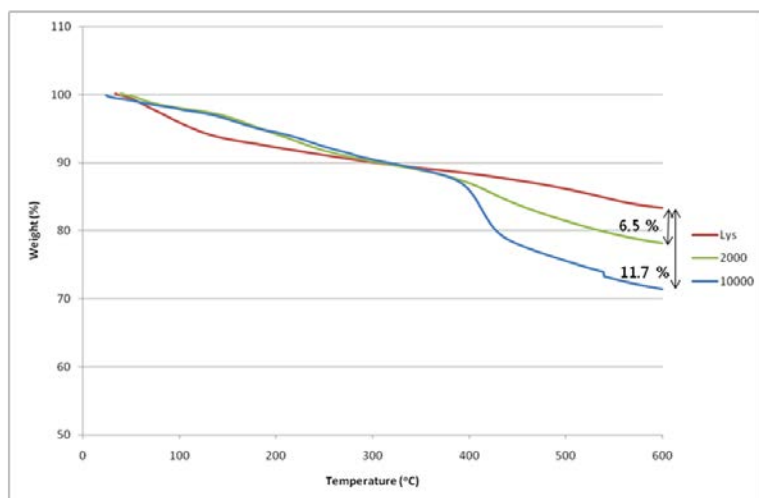
**(a)**



**(b)**



**Figure 3.5.** TEM images of PEGylated F-silica NPs, with  
(a) PEG<sub>2000</sub>, and (b) PEG<sub>10000</sub>.



**Figure 3.6.** The results of TGA Analysis Data of PEG Modified F-silica NPs

### 3.2.3. Preparation and Characterization of Multifunctional F-silica NPs

Optical imaging with PET has the potential for providing better spatial resolution with anatomical information and also improved signal sensitivity. For combination of imaging modalities, optical imaging and PET, we designed dual modal imaging probe by conjugation of F-silica NPs with  $^{68}\text{Ga}$ -NOTA.

PET uses positrons to create  $\gamma$ -rays. The  $^{68}\text{Ga}$  is a positron emitting molecule with a short half-life (67.6 min). Its short half-life and hydrophilic nature are adequate in labeling NPs for rapid clearance for PET. The importance of  $\text{Ga}^{68}$  for clinical PET has been increased recently.<sup>25</sup> In order to introduce  $^{68}\text{Ga}$  on the NPs, thiocyanate group containing macrocyclic chelating agent NOTA was attached to the amino group on PEGylated F-silica NPs. NOTA is a 9-member cyclic compound and has been reported to form a highly stable neutral complex with  $\text{Ga}^{3+}$  ion, which is inert even in 6 N nitric acid.<sup>26</sup>

Also, we investigated multifunctional F-silica NP for targeting and imaging by employing anti-body. In order to conjugate antibody, a water soluble linker, sulfo-SMCC, was coupled to the PEGylated F-silica NPs. NOTA and sulfo-SMCC were attached to the F-silica NPs surface competitively with different mechanism. For specific immobilization of antibody, a maleimide moiety of SMCC was

introduced through covalent linkage with F-silica NPs. The maleimide moiety can selectively react with sulfhydryl group. To introduce sulfhydryl residue on Herceptin, the antibody, which originally contains disulfide linkages at the hinge region, was reduced with MEA. The sulfhydryl groups produced by this method can couple to the maleimide moiety of sulfo-SMCC on F-silica NPs. Therefore, we expect that the functionalized F-silica NP is capable of targeting cell, and also detectable by optical and PET imaging. Table 3.2 shows the size and the zeta potential of these particles. The size of NOTA and SMCC modified F-silica NPs were 117.9 nm in diameter, as determined by dynamic light scattering (DLS), and the zeta potential was -18.6 mV.

In addition, we investigated the effects of PEG chain length and the amount of amine moiety (% APTS, v/v) on the resulting particle size and surface charge. The results are summarized in Table 3.2, which show PEG<sub>2000</sub> modified F-silica NPs is smaller than PEG<sub>10000</sub> modified F-silica NPs. However, both of them have negatively charged.

On the other hand, the size of PEG<sub>10000</sub> modified F-silica NPs have larger size than APTS (1%,v/v) treated one. They also have negative charge on the surface. The negative charge on their surface can be attributed to a small amount of remnant anionic surfactant used in the synthesis of F-silica NPs.

The net charge of nanoparticles has a pronounced effect on their behavior according to the surrounding environment. Furthermore, it can have influence on the adsorption of different physiological lipoproteins

in systemic circulation and plays a critical role in the clearance of the nanoparticles from the animal body.<sup>27</sup>

**Table 3.2.** Size and Zeta Potential of Multifunctional F-silica NPs

Modified F-silica Nanoparticles	Size (nm)	Zeta potential (mV)
APTS(5 v/v%)-(Lys) <sub>2</sub> -PEG <sub>2000</sub> -Lys-NOTA/SMCC	117.9	-18.6
APTS(5 v/v%)-(Lys) <sub>2</sub> -PEG <sub>2000</sub> -Lys-NOTA/SMCC	88.4	-16.5
APTS(5 v/v%)-(Lys) <sub>2</sub> -PEG <sub>10000</sub> -Lys-NOTA/SMCC	147.6	-16.7
APTS(1 v/v%)-(Lys) <sub>2</sub> -PEG <sub>10000</sub> -Lys-NOTA/SMCC	89.2	-5.31



### 3.2.4. Radio-labeling of Surface Modified F-silica NPs

We studied  $^{68}\text{Ga}$  labeling efficiency of F-silica NPs for PET imaging. The labeling procedure, including purification, was straightforward and the products were analyzed by ITLC-SG (Instant Thin Layer Chromatography Silica Gel) eluted with 0.1 M citric acid. Free  $^{68}\text{Ga}$  did not move at all and  $^{68}\text{Ga}$  labeled F-silica NPs moved with the eluting solvent front.

We investigated the effects of PEG chain length and the amount of amine moiety (% APTS, v/v) on the  $^{68}\text{Ga}$  labeling efficiency

In case of PEG 2000 conjugated F-silica NPs,  $^{68}\text{Ga}$  labeling efficiency was 77.28 % and then reached to 96.5 % after purification. However, Herceptin immobilized ones gave 31.56 % of labeling efficiency. This result demonstrates that Herceptin conjugation interferes with NOTA, which has decreased Ga labeling efficiency.

We also tried to figure out the effect of PEG chain length on labeling efficiency. When long chain PEG (MW 10,000) was conjugated to F-silica NPs to improve the solubility and the stability, the resulting F-silica NPs gave 49.8 % of Ga labeling yield.

In that case of APTS (1%, v/v) the ones with modified F-silica NPs, which have less amount of amine moiety than using APTS (5%, v/v), the labeling efficiency was 89.53 %, and after purification, it was increased to 95.93 %. These results demonstrate that APTS(1%, v/v), modified F-silica NPs conjugated with PEG 10,000 is an effective

surface modification method for  $^{68}\text{Ga}$  labeling. Therefore, functionalized F-silica NPs are promising candidate as an efficient PET imaging probe.

**Table 3.3.**  $^{68}\text{Ga}$  labeling Efficiency of Multifunctional F-silica NPs

Modified F-silica Nanoparticles	$^{68}\text{Ga}$ labeling efficiency(%)		
	after 30 min.	after washing	
		precipitated	supernatant
APTS(5 v/v%)-(Lys) <sub>2</sub> -PEG <sub>2000</sub> -Lys-NOTA/SMCC	77.28	96.51	79.22
APTS(5 v/v%)-(Lys) <sub>2</sub> -PEG <sub>2000</sub> -Lys-NOTA/SMCC	31.56		
APTS(5 v/v%)-(Lys) <sub>2</sub> -PEG <sub>10000</sub> -Lys-NOTA/SMCC	49.84		
APTS(1 v/v%)-(Lys) <sub>2</sub> -PEG <sub>10000</sub> -Lys-NOTA/SMCC	89.53	95.93	93.68

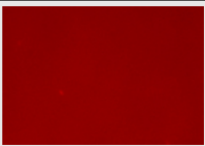
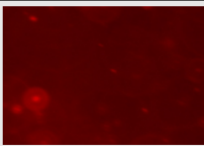
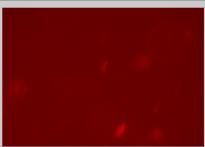

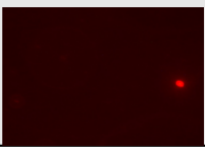
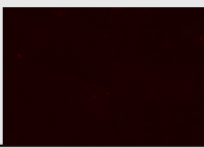
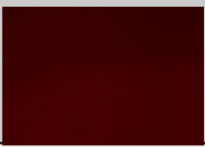
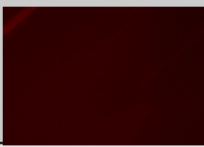
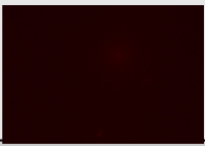
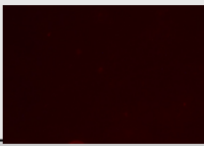
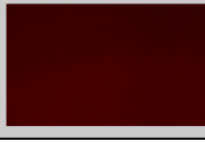
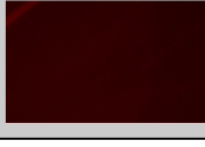
**Table 3.4.** The Results of DLS Analysis of Multifunctional F-silica NPs after  $^{68}\text{Ga}$  labeling

Modified F-silica Nanoparticles	Size (nm)	
	Size (nm)	after $^{68}\text{Ga}$ labeling
APTS(5 v/v%)-(Lys) <sub>2</sub> -PEG <sub>2000</sub> -Lys-NOTA/SMCC	117.9	117.6
APTS(5 v/v%)-(Lys) <sub>2</sub> -PEG <sub>2000</sub> -Lys-NOTA/SMCC	88.4	108.7
APTS(5 v/v%)-(Lys) <sub>2</sub> -PEG <sub>10000</sub> -Lys-NOTA/SMCC	147.6	134.2
APTS(1 v/v%)-(Lys) <sub>2</sub> -PEG <sub>10000</sub> -Lys-NOTA/SMCC	89.2	167.2

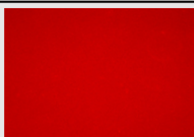

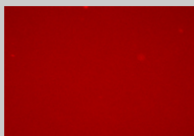

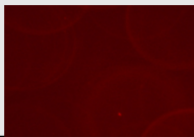
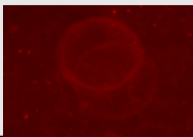
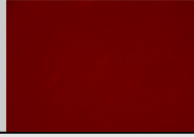

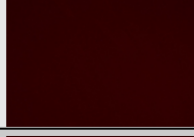
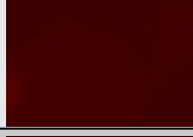


### 3.2.5. Aggregation Studies of Multifunctional F-silica NPs

There is a natural tendency for the nanoparticles to aggregate through hydrophobic interactions or attractive van der Waals forces in an effort to minimize the surface energy. Therefore, it is important to keep the nanoparticles suitably dispersed in an aqueous environment for bio application. The ideal NPs must fulfill a number of stringent requirements: it should be easily dispersible and stable (i.e., resistant to aggregation) in a variety of local *in-vivo* environments and not be affected by differences in solvent polarity, ionic strength, pH, or temperature. It should exhibit limited nonspecific binding and be resistant to reticulo endothelial system (RES) uptake, and have sufficiently long circulation time in the blood stream for long term quantitative imaging. To fulfill these terms, we introduced negatively charged ligand THPMP on the F-silica NPs and further modified them with PEG. The aggregation tendency of multifunctional F-silica NPs at different concentrations was observed by using CLSM. Figure 3.7 shows the images of dispersed multifunctional F-silica NPs. Both of PEG<sub>2000</sub> and PEG<sub>10000</sub> conjugated multifunctional F-silica NPs showed well dispersed condition. Aggregation of NPs with biological molecules via electrostatic interactions could be a serious issue. Therefore, its minimization is essential for sensitive detection of targeted proteins.<sup>28</sup>

(a)

F-silica NPs concentration	solvent	DPBS	
	temperature		After sonication
1 mg/mL	RT		
	4°C		
250 µg/mL	RT		
	4°C		
62.5 µg/mL	RT		
	4°C		

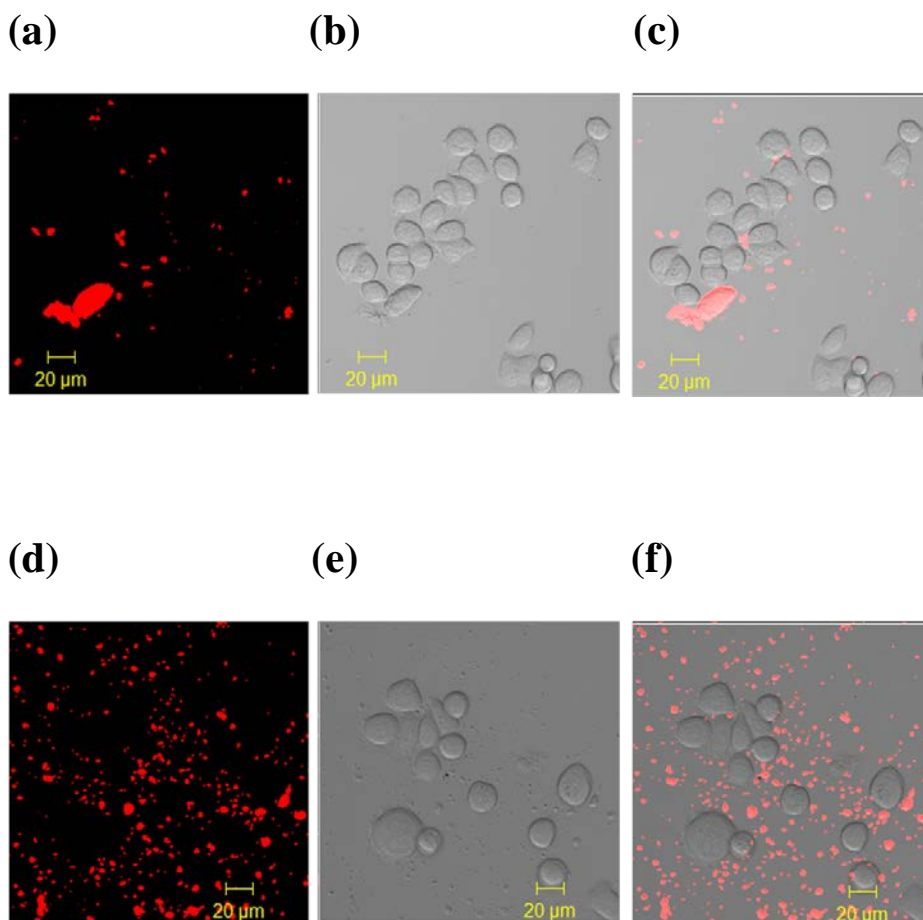
(b)

F-silica NPs concentration	solvent	DPBS	
	temperature		After sonication
1 mg/mL	RT		
	4°C		
250 µg/mL	RT		
	4°C		
62.5 µg/mL	RT		
	4°C		

**Figure 3.7.** The CLSM Images of Dispersed Multifunctional F-silica NPs; (a) Conjugated with PEG<sub>2000</sub> (b) Conjugated with PEG<sub>10000</sub>

### **3.2.6. *In vitro* Cellular Binding Study**

HER2, human epidermal growth factor receptor-2, is a potential target as a diagnostic biomarker for breast and ovarian cancers. HER2 over expressing breast cancer cells, SK-BR-3, were incubated with the same concentration (300 µg/ 30µL) of trastuzumab immobilized F-silica NPs. Trastuzumab, a humanized monoclonal antibody, binds to HER2 receptor specifically. The primary goal of antibody conjugation is to introduce a targeting moiety to the F-silica NPs. However, as shown in Figure 9, the PEG 2000, or PEG 10000 conjugated F-silica NPs did not bind the cell receptor, respectively. These results demonstrate that antibody conjugation to a nanoparticle without consideration for the recognition site can shield the binding regions and reduce the targeting properties.



**Figure 3.8.** Confocal Images of Functionalized F-silica NPs conjugated with (a) PEG 2000 (d) PEG 10,000  
Optical images of SKBR3 cell images (b),(e), and merged images (c),(f)

## Conclusion

The fluorescent dye-doped silica nanoparticles(F-silica NPs) as the core material of optical imaging probe were synthesized through reverse microemulsion method, which gave highly spherical, monodispersed nanoparticles. For fabrication of dualmodal imaging probe for PET imaging, we prepared  $^{68}\text{Ga}$  conjugated F-silica NPs. These particles showed the effective Ga labeling efficiency which proved to be a good candidate for efficient PET imaging probe.

In addition, F-silica NPs were conjugate with PEG and measured the effect of PEG chain length on the resulting particle's size, surface charge and  $^{68}\text{Ga}$  labeling efficiency. The results showed that APTS (1%,v/v) modified F-silica NPs conjugated with PEG 10,000 gave effective  $^{68}\text{Ga}$  labeling.

Furthermore, as a targeted imaging agent for breast cancer, we prepared Herceptin conjugated F-silica NPs using water soluble liker. However, these NPs did not bind to the cell receptor. Further improvement of antibody conjugation for effective targeting without losing its functionality is necessary.



## 초 록

나노 입자들은 생체영상분야에서 영상을 위한 표지자나 생물학적 현상을 영상화할 수 있는 추적자로서 활발하게 이용되고 있다. 최근에는 생체영상기술의 발전으로 인해 특정 암에 대한 특이적인 표지자를 추적하여 초기 암 진단과 치료에 이용되고 있다. 생체영상분야에서 이용되고 있는 다양한 영상기술들은 각각 장점과 단점을 갖고 있으며, 진단 목적에 따라 다르게 이용되고 있다. 그러나, 한 가지의 영상 기술만으로는 의학적인 진단에 있어서 부족함이 따른다. 이를 위해 둘 혹은 세 가지의 영상기술을 접목하여 더 많은 의학적 정보와 생물학적 현상을 분석하는 노력이 많이 이루어지고 있다. 이에 본 연구에서는 광학 영상과 핵 의학영상 기술을 결합하여 생체조직을 손상시키지 않으면서, 기존 영상 기술보다 민감하게 신호를 얻어 낼 수 있는 나노 표지자의 개발을 시도하였다. 먼저, 형광이 담지된 실리카 나노 입자를 합성하여 광학영상을 얻을 수 있도록 설계하였으며, 실리카 나노 입자 표면에 방사선 동위원소인  $^{68}\text{Ga}$ 을 표지하여 핵 의학 영상인, PET 영상이 가능하도록 하였다. 또한 특정암에 대한 진단이 가능하도록 특이적인 항체를 결합시켜 하나의 나노 입자를

이용하여 초기암 진단에 있어서 광학 영상과 핵 의학 영상이 동시에 가능하도록 설계하였다. 또한 이를 생체 내에서의 이용이 가능하도록 친수성 고분자인 polyethyleneglycol(PEG)을 표면에 붙여 생체적합성을 증가시킬 수 있도록 하였다. 이때 PEG의 분자량을 2000,10000 으로 달리 도입하여, PEG 사슬 길이에 따른 나노입자의 사이즈와 표면의 전하의 변화 등 나노 입자의 물성을 확인하였다. 이러한 과정을 통해 광학 영상과 핵 의학 영상을 동시에 구현할 수 있는 나노표지 입자의 가능성을 엿볼 수 있었다.

**주요어:** 다기능성 나노입자, 형광담지실리카나노입자, 특이적 표적을 위한 영상 표지자, 표면처리, 광학영상, 핵의학영상

**학 번:** 2010-22665

## References

1. JK Willmann, N van Bruggen, LM Dinkelborg, Gambhir. Molecular imaging in drug development. *Nature Reviews Drug Discovery*, **2008**, 7, 591-607
2. Z Liu, F Kiessling, J Gätjens. Advanced Nanomaterials in Multimodal Imaging: Design, Functionalization, and Biomedical Applications. *Journal of Nanomaterials*, **2010**, Article No. 51
3. R Weissleder, MJ Pittet. Imaging in the era of molecular oncology. *Nature*, **2008**, 452, 580-589
4. M Glaser, SK Luthra, F Brady. Application of positron-emitting halogens in PET oncology. *International journal of oncology*, **2003**, 22, 253-267
5. J Cheon and JH Lee. Synergistically integrated nanoparticles as multimodal probes for nanobiotechnology. *Accounts of Chemical Research*, **2008**, 41, no. 12, 1630-1640,.
6. H Koo, IC Sun, JH Ryu, K Kim, IC Kwon. Multifunctional nanoparticles for multimodal imaging and theragnosis. *Chemical Society Reviews*, **2012**, 41, 2656-2672
7. N Sanvicens, MP Marco. Multifunctional nanoparticles properties and prospects for their use in human medicine. *Trends Biotechnol* .**2008**. 26(8),425-433

8. VK Varadan, L Chen, and J Xie. Nanomedicine: Design and Applications of Magnetic Nanomaterials, *Nanosensors and Nanosystems*, Wiley, London, UK, 2008.
9. HN Wagner, Z Szabo, JW Buchanan. Principles of Nuclear Medicine, W. B. Saunders, Philadelphia, Pa, USA, 2<sup>nd</sup> edition, 1995.
10. P Tallury, K Payton, S Santra. Silica-based multimodal/ multifunctional nanoparticles for bioimaging and biosensing applications. *Nanomed.* **2008**,3(4),579–592
11. P Sharma, S Brown, G Walter, S Santra, Brij Moudgila. Nanoparticles for bioimaging. *Advances in Colloid and Interface Science*,**2006**,123–126,471–485
12. M Wang, M Thanou. Targeting nanoparticles to cancer. *Pharmacological Research*,**2010**, 62, Issue 2,90–99
13. X Montet, M Funovics, K Montet-Abou, R Weissleder, L Josephson. Multivalent effects of RGD peptides obtained by nanoparticle display. *J Med Chem.* **2006**, 49, 6087-93.
14. CE Ashley, EC Carnes, GK Phillips, D Padilla, PN Durfee, PA Brown, et al. The targeted delivery of multicomponent cargos to cancer cells by nanoporous particle-supported lipid bilayers. *Nat Mater.* **2011**, 10,389-97.
15. W Tan, K Wang, X He, XJ Zhao, T Drake, Lin Wang, Rahul P. Bagwe, Bionanotechnology based on silica nanoparticle. *Medicinal Research Reviews*.**2004**,24, 621–638

16. J Cheon, JH Lee. Synergistically integrated nanoparticles as multimodal probes for nanobiotechnology. *Accounts of chemical research*, **2008**, 41 (12), 1630–1640
17. S Jiang, Muthu Kumara Gnanasammandhan, Yong Zhang. Optical imaging-guided cancer therapy with fluorescent nanoparticles. *J. R. Soc. Interface*. **2010**, 7, 3-18
18. M Liong, J Lu, M Kovochich, T Xia, SG Ruehm, AE Nel. Multifunctional inorganic nanoparticles for imaging, targeting, and drug delivery. *ACS Nano* .**2008**, 2(5):889–896
19. SM Moghimi, AC Hunter, JC Murray. Long-circulating and target-specific nanoparticles: Theory to practice. *Pharmacol Rev.* **2001**, 53,283-318.
20. J Xie, C Xu, N Kohler, Y Hou, S Sun. Controlled PEGylation of monodisperse Fe<sub>3</sub>O<sub>4</sub> nanoparticles for reduced non-specific uptake by macrophage cells. *Adv Mater.* **2007**, 19, 3163-6.
21. S Santra, HS Yang, D Dutta, T Jessie, Stanley, H Paul, Holloway, W Tan, M Brij, Moudgil, A Robert. Mericle. TAT conjugated, FITC doped silica nanoparticles for bioimaging applications. *Chem. Commun.*, **2004**,24, 2810-2811
22. RP Bagwe, LR Hilliard, W Tan. Surface modification of silica nanoparticles to reduce aggregation and nonspecific binding. *Langmuir*, 2006, 22 (9), 4357–4362
23. R Gref, Y Minamitake, MT Peracchia, V Trubetskoy, V Torchilin, R Langer. Biodegradable long-circulating

- g polymeric nanospheres. *Science*. **1994**, 263, 1600
24. DE Owens, NA Peppas. Opsonization, biodistribution and pharmacokinetics of polymeric nanoparticles. *International journal of pharmaceutics*, **2006**, 307(1), 93–102
  25. Roesch, J Frank, Riss, Patrick. The Renaissance of the  $^{68}\text{Ge}/^{68}\text{Ga}$  Radionuclide Generator Initiates New Developments in  $^{68}\text{Ga}$  Radiopharmaceutical Chemistry. *Current Topics in Medicinal Chemistry*, **2010**, 10, 1633–1668
  26. JM Jeong, MK Hong, YS Chang, YS Lee, YJ Kim, GJ Cheon, DS Lee, JK Chung, MC Lee. Preparation of a promising angiogenesis PET imaging agent:  $^{68}\text{Ga}$ -labeled c(RGDyK)-isothiocyanatobenzyl-1, 4, 7-triazacyclononane-1, 4, 7-triacetic acid and Feasibility Studies in mice. *J Nucl Med*. **2008**, 49, 830–836
  27. HS Choi, L Wenhao, M Preeti, T Eiichi, John P Zimmer, Binil Itty Ipe, Mouni G Bawendi, John V Frangion. Renal clearance of Quantum dot. *Nature Biotechnology*. **2007**, 25, 1165 - 1170
  28. OV Salata. Application of Nanoparticles in biology. *Journal of nanobiotechnology*, **2004**, 2, 3

## Acknowledgement

유기합성실을 떠난 지 벌써 1년이 지나고서야 이렇게 석사과정을 마치게 되었습니다. 2년 동안 유기합성실에서 너무나 많은 것을 배우고 느끼고 경험하였습니다. 어렵게 석사과정을 마무리 한 만큼 주변에서 너무나 많은 도움을 받은 것 같습니다. 글로나마 감사의 마음을 전합니다.

먼저, 너무나 많은 가르침을 주신 이윤식 교수님. 정말 감사합니다. 교수님의 제자라는 것이 저에게는 너무나 감사한 일이고, 큰 행운인 것 같습니다. 전공에 관한 지식뿐만 아니라 인생을 살아가는 지혜들을 많이 배웠습니다. 너무나도 존경하는 우리 교수님. 저의 인생에 있어서 교수님을 만날 수 있었다는 것만으로도 저의 석사과정은 너무 뜻 깊은 시간이었던 것 같습니다. 항상 건강하시고 앞으로도 멋진 모습, 지금의 열정적인 교수님 모습, 오래오래 볼 수 있었으면 좋겠습니다. 교수님 사랑해요

사랑하는 우리 엄마, 아빠. 내가 살아가는 힘. 딸 공부시키느라 고생 많이 했지. 힘들어도 내색 안하고 언제나 딸 위해 삶을 사는 우리 엄마아빠. 앞으로도 좋은 딸 멋진 딸 될게. 이렇게 잘 키워줘서 너무 감사해요. 사랑해.

우리 실험실 식구들. 나의 사수 멋진 호만 오빠. 오빠 덕분에 2년 동안 많이 배웠어요. 석사과정 시작과 끝 모두 오빠의 도움이 없었다면 저의 지금은 없었을 거예요. 항상 열정적인 호만오빠. 제가 오빠 좋아하는 거 아시죠? 나의 멋진 선배.

존경합니다.

나의 멘토 선영언니. 언니는 정말 멋진 여자에요. 석사 하면서 언니 덕분에 힘들었던 시간들 견딜 수 있었어요. 언니의 모습을 보면서 많이 본 받고 배우려고 노력했던 것 같아요. 언니한테는 실망시켜드리기 싫었는데.. 그래도 이렇게 졸업을 합니다. 언니 너무 감사해요. 사랑해요 히히

나의 영원한 오빠 형석오빠. 오빠!!! 오빠 덕분에 석사과정 웃으며 즐기며 무사히 보낼 수 있었어요. 힘들 때마다 오빠가 곁에서 조언도 해주시고, 좋은 얘기 많이 해주셔서 제가 이렇게 좋은 회사에 온 것 같아요. 저의 정신적 지주예요 오빠는 ^^ 감사해요.

그리고 멋진 아기 아빠 홍준오빠 같이 졸업하게 되서 기뻐요 오빠는 우리 실험실의 감초^^. 항상 묵묵히 챙겨주시고 신경 써주셨던 재희오빠 세심한 부분 챙겨 주셨던 거 걱정해주시고 마음 써주셨던 거 너무 감사해요 오빠. 나의 멋진 동기 오빠들. 나쁜 남자 산오빠. 오빠 때문에 석사 하면서 많이 울기도 웃기도 한 거 같아. 덕분에 많이 배웠어 고마워^^ 똑똑한 요한오빠. 오빠를 보면서 석사 하는 동안 자극을 많이 받은 것 같아. 동기 오빠들. 나를 웃으며 울며 2년 동안 정 많이 든 것 같아. 고맙고 미안해^^

나의 사랑 새롭이, 진경이. 너희들 없었으면 나의 2년은 어땠을까. 말로 표현 못할 만큼 너희들의 존재는 너무나 고맙고 너희들이 내 친구라는 건 너무 큰 복이다. 너희들 때문에 힘들었던 시간 견딜 수 있었고, 작은 것에도 감사하고 행복해 하면서 석사과정 할 수 있었어. 너무 고마워. 회사다니한다고 자주 만나지도 못하고 연락도 잘 못하고 미안해. 졸업할 때까지 우리 진경이한테는 완전 애물단지다. 그치? 너무 고맙고 미안해. 우리 새롭이 진경이 너무나 고맙고 사랑해. 영원히 함께 하자.

나의 멋진 선배들. 용선오빠. 성원오빠. 태규오빠. 송언니. 선



배들과 함께 했던 일년은 너무너무 즐거웠었어요. 선배들 덕분에 많이 웃으며 보냈던 것 같아요. 감사합니다. 든직한 준혁이. 귀염둥이 영오. 너희들과 함께 식사하면서 많이 즐거웠던 것 같아. 많이 챙겨주지 못해 미안해. 너희들이 많이 도와주고 함께해줘서 잘 마무리 하는 것 같아. 준혁이 여태 해왔던 것처럼 앞으로 멋지게 박사과정 잘 해내고. 우리 귀염둥이 영오. 영오가 항상 누나한테 살갑게 대해주고 잘해줘서 너무 고마웠어. 앞으로도 멋진 모습 기대할게! 그리고 세원이. 많은 시간을 함께 하지

세계최고 편광판팀. 먼저, 부족한 저를 우리 팀의 구성원으로 뽑아주신 우리 위원님. 기회를 주시고 믿고 지켜봐 주셔서 감사합니다. 앞으로 더 잘할 수 있도록 노력하겠습니다. 우리 팀 기동 남과장님. 부족한 저를 항상 응원해주시고 격려해주셔서, 이렇게 졸업할 수 있게 되었습니다. 앞으로는 더 좋은 모습 보여드릴 수 있도록 할게요. 지금은 열심히 공부 중인 나의 멘토 권과장님. 과장님 덕분에 회사생활 잘 적응한 것 같아요. 너무나 배울 점이 많은 우리과장님. 과장님께서 항상 졸업 걱정해주시고 응원해주셔서 많은 힘이 되었습니다. 감사합니다. 멋진 김과장님. 졸업 때문에 연수 늦게 가느라 민폐 끼치고.. 죄송해요 과장님^^ 제가 과장님 좋아하는 거 아시죠? 저의 정신적 지주 정대리님. 대리님의 조언들 덕분에 너무 큰 힘이 되었습니다. 졸업 때문에 많이 걱정하면서 일했는데 대리님이 응원해주셔서 잘 마무리합니다. 앞으로도 잘 부탁드려요^^ 저의 버팀목 남대리님. 일에서나, 생활에서나 걱정 많이 해주시고 신경 써주시고 응원해주신 덕분에 이렇게 졸업할 수 있게 되었어요. 연수 가느라 민폐 끼쳐서 죄송해요 우리대리님 최고 ^^\* 나의 사랑하는 동기 혜민언니, 미린이. 언니랑 미린이가 곁에 있어 너무나 큰 힘이고 복이야. 너무너무 고마워. 힘들 때마다 둘의 존재가 더 감사해. 알라뷰.

내사랑 지혜, 지선이. 나 드디어 졸업이다. 너희들과 이 영광 함께 하고 싶다. 응원해줘서 고마워.

제 인생에 있어 뜻 깊은 2년. 어렵게 석사과정 마무리 하는 만큼 더 소중한 것 같습니다. 주변의 좋은 사람들 덕분에 잘 마무리 할 수 있었고, 더더욱 값진 시간이었습니다. 너무 감사합니다.